Advanced Materials Research Vol. 59 (2009) pp 158-163
online at http://www.scientific.net

Micromechanical Model Of Interface Between Fibre And Matrix Of Metal Matrix Composite Reinforced With Continuous Fibre

A. Ríos[1,a] and A. Martín-Meizoso[1,b]

[1]CEIT and Tecnun (University of Navarra), E-20018 San Sebastián, Spain

[a]arios@ceit.es, [b]ameizoso@ceit.es

Keywords: Copper matrix, modelling, interface, cohesive model.

Abstract. A micromechanical model is employed to investigate the influence of the interface between the fibre and the matrix of a metal matrix composite with long fibre, which is elaborated through finite element method. Also, transverse properties of composite are studied in the present work. The interface, between the fibre and the matrix, is studied employing cohesive elements. These elements employ a cohesive zone model, which follows a bilinear law.

Introduction

New composite materials have been developed to be used as heat sink for high temperature applications, for instance, as inside-wall of a thrusters chamber and as a component of divertor. These composite materials must show excellent thermal conductivities as well as they should be able to keep its original shape and strength when subjected to thermal and mechanical loads [1]. Many investigations have been developed employing the micromechanical modelling to understand the mechanical and thermal behaviour. Fibre shows elastic behaviour and matrix shows creep behaviour, when composite undergoes high temperature [2]. Thus, the composite material should be able to carry fatigue and creep. A good performance of the composite materials depends on a good adhesion at the interface, between fibre and matrix. Even though, composite materials can be design with a high strength in the fibre direction, it is not always possible to avoid that the composite undergoes transverse loadings [3]. Additionally, composite materials develop thermal stresses during thermal cycling. These stresses can be relaxed in different ways: i) plastic deformation of the ductile matrix, ii) cracking of fibres and iii) debonding of interface between the fibre and the matrix [4-6]. Several authors have considered a perfect interface [7, 8] and imperfect interface [9-17] to study the interface behaviour of the composites materials. Contact surface with residual stresses have been used by Nimmer, Ding and Bowen to study the interface behaviour [10,11,15]. Wisnom developed interface elements to study the transverse tensile properties of the composites [13]. These elements consider pairs of nodes on each side of the interface coupled with stiff springs until the stresses reach a predefined failure criterion. A quadratic equation is used as criterion of failure of the interface. The aforementioned analysis criterions neglected to use a thickness of interface. On another hand, L. L. Shaw and D. B. Miracle [9] suggest to use an independent interface with thickness. Also, Aghdam and Falahatar [17] used two type of interfaces to study the interface behaviour: fibre-coating and coating-matrix. Finally, cohesive zone model (CZM) is a method widely used to analyse the failure of the interface. This model considers an infinitely thin interface [18,19]. Zhang et al. have employed a cohesive model that obeys a traction-displacement law. There are different cohesive models: lineal, exponential or trapezoidal. Micromechanical modelling is used to study the composite material; and cohesive elements are employed to analyse the transversal behaviour, as well as the effects of the failure at the interface. The analysis takes into account the residual stresses, volume fraction and different distributions for the fibres.

Finite Element Model

Boundary Conditions. Since the present work is focused on the analysis of the transverse properties of the composite materials, generalized plane strain elements are used to model composites with long fibre. These elements represent a situation where the length of fibre is longer than the diameter of the fibre [4]. Variations of stresses and strains, along fibres, are assumed to be zeros [13]. The two-dimensional model uses "CPEG4" elements. The boundary conditions for a square arrangement are shown in fig. 1. The nodal displacement of the left side is constrained in the "x" direction, and the nodes of the bottom side are constrained in the "y" direction. The nodes of the upper side have identical displacement in the "y" direction. Similarly, the nodes on the right edge have equal displacement [4,8-10,13,15,17]. The analyses have been calculated using ABAQUS© finite element software [20].

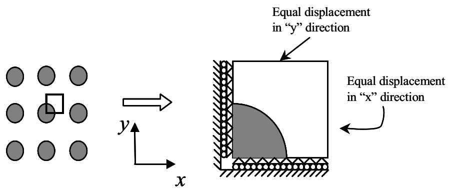

Figure 1. Boundary conditions for a square arrangement of fibres

Interface Model. The constitutive equation of the interface are developed in a phenomenological way, it means, that constitutive equations satisfied an empiric relation obtained from experimental results [21]. The micromechanical modelling uses a cohesive model with linear law. The cohesive model is shown in figure 2. The thickness of the element is neglected. Cohesive elements (COH2D4) are introduced between the fibre and the matrix. The cohesive elements permit to know the initial damage and its propagation. Data required for cohesive elements are obtained from push-out tests [22]. The traction-displacement relation, of the linear law, is based on the mechanic of the fracture. Thus, the area of the triangle, limited by the traction-displacement curve, is equal to energy released (G^c) by the separation of interface [23]. The cohesive law does not account for damage in compression. The damage starts when the failure criterion is satisfied. Nominal quadratic stress is the failure criterion used in the cohesive elements.

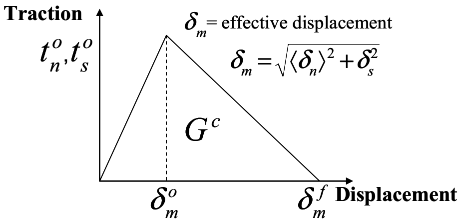

Figure 2. Cohesive law model

$$\left\{\frac{\langle t_n \rangle}{t_n^o}\right\}^2 + \left\{\frac{t_s}{t_s^o}\right\}^2 = 1 \quad (1)$$

where: t_n= normal component of stress, t_s= shear component of stress, $\langle t_n \rangle = \frac{1}{2}(t_n + \|t_n\|)$.

The "power law criterion" is the most widely used to predict the damage propagation under mix mode loading, which is establish as an interaction between energy release rates [24]. The damage evolution is based in the energy released, which is dissipated as a result of the damage process, also called fracture energy. The energy of fracture is equal to the area under the traction-displacement curve. The power law criterion establishes that the failure condition, in mix-mode, is governed by a power law interaction of energies.

$$\left\{\frac{G_n}{G_n^C}\right\}^\alpha + \left\{\frac{G_s}{G_s^C}\right\}^\alpha = 1 \quad (2)$$

where: G_n= normal adhesion energy, G_t =shear adhesion energy, G_n^c=critical normal adhesion energy, G_t^c= critical shear adhesion energy.

The transverse and shear traction shall be the same value due to the lack of experimental data. The maximum resistance (t_n, t_s) and the effective displacement (δ_m), define the fracture behaviour at the interface. The properties required to define the fracture behaviour are the following: stiffness of the element (K), the toughness to fracture (G_n^c, G_s^c), the normal stress (t_n), and the shear stress (t_s). Energy adhesion values between the fibre and the matrix have been calculated from push-out test, for simplicity, $G_n^c = G_s^c$. The equation used is the following [25]:

$$G_n^c = \frac{B_2 R_f}{E_f}\left[\frac{(\tau_d - \tau_s)t}{R_f}\right]^2 \quad (3)$$

where: G_n^c = interface toughness (J/m^2), τ_d = debond shear stress (MPa), τ_s = interphase shear stress (MPa), t = specimen thickness (m), B_2 = no-dimensional constant, R_f = fibre radius (m), E_f = Young´s modulus of the fibre (MPa).

Material properties

The composite system studied is formed by a copper matrix and long fibres of silicon carbide (SCS-6). SiC fibre is considered to behave elastically and the matrix is considered as elastic-plastic. The diameter of the fibre is 140 µm. The coefficients of Poisson are 0.3 and 0.25 for Cu and SiC respectively. The properties of the fibre and the matrix are temperature dependent. Both, fibre and matrix, are considered isotropic and homogeneous. Since most of metals undergo creep at temperatures in excess of one half of their melting points, creep behaviour has been incorporated in the copper matrix as a user subroutine, with a potential power law. The potential law used to describe the creep behaviour is:

$$\dot{\varepsilon} = A\sigma^n \exp\left(\frac{Q}{RT}\right) \quad (4)$$

where: $\dot{\varepsilon}$ = creep strain rate, σ = stress (N/m^2), Q = activation energy, R = constant of gas, T = absolute temperature (K), n = exponent, A = constant MPa^{-1}

Results and discussion

The composite materials develop residual stresses when cooling from the manufacture temperature to room temperature, due to the differences on the thermal coefficient of expansion, between the fibre and the matrix. Therefore, the present model takes into account a cooling from 900 to 20 ºC. Uniform temperature distribution is assumed in the unit cell. The radial stresses are measured around the fibre, starting at the bottom right-hand side of the model. The direction of angle (θ) is shown in fig. 3 with zero at the bottom edge. Distribution of compressive radial stresses, which have been developed in the interface (between the fibre and the matrix, at 20ºC), are shown in fig. 4. The maximum compressive radial stress (square arrangement of fibres) is 21.6 MPa at 0 and 90 degrees, and the minimum compressive radial stress is 20.75 MPa. On other hand, the residual stresses for an hexagonal arrangement of fibres is 21.7 MPa at 0 and 60ºC, and 22.85 MPa at 30 and 90 º. The maximum radial stresses, in a hexagonal arrangement of fibres, are slightly greater than radial stresses for square arrangement of fibres. The tensions generated, between the fibre and the matrix during the heating of the composite, are not enough to cause debond of the interface. For the case of a square distribution of fibres, the maximum radial tension is 7.3 MPa at 0 and 90 degrees (with 30% of SiC fibre, at 550 ºC). Fig. 5 shows the contours maps for square and hexagonal arrangement at 550 ºC.

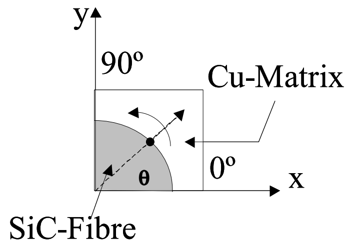

Figure 3. Schematic diagram for radial stress

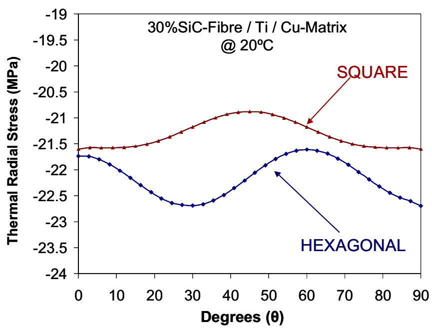

Figure 4. Distribution of compressive radial stress at interface for two fibre arrangements: square and hexagonal (30%SiC$_f$)

Transversal mechanical loading. The transverse mechanical loading is applied to the unit cell by means of a nodal displacement. All nodes from the right edge have the same displacement. These nodes are tied to a reference node, which is displaced. The stresses and strains of the unit cell can be obtained by averaging integration points of the elements:

$$\bar{\varepsilon} = \frac{1}{V}\int \varepsilon \, dV \qquad \bar{\sigma} = \frac{1}{V}\int \sigma \, dV \ . \tag{5}$$

The separation, between the matrix and the fibre is located at 0 degrees (at room temperature) for a square arrangement of fibres. The interface debonding, with a hexagonal distribution of fibres, ranges from 0 to 27 degrees. Although the debonding stars, the tension distributions are not enough to propagate around the fibre. On the other hand, the interface can be improved when a titanium layer is incorporated between the SiC-fibre/Cu-matrix interface, thereby, the transverse strength increase from 10 MPa to 50 MPa before the damage criterion is satisfied.

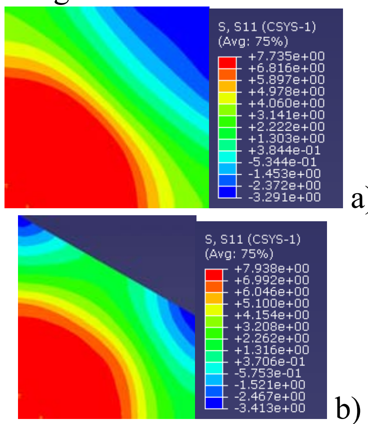

Figure 5. Contours maps of the radial thermal stress at 550 ºC ($30\%SiC_f$): a) square, b) hexagonal

Effect of distribution and volume fraction of fibre in the matrix. As shown in fig. 6, the transverse elongation, of the composite, decreases when the volume fraction of fibres increase from 30 to 40%, before the interface starts to debond. The interface debonding starts when stress reaches 44.1 MPa and 41.2 MPa (after interface elements have satisfied the failure criterion) for a square and hexagonal arrangement of fibres respectively, both at room temperature (it means, that the power law criterion (established for delamination propagation) has been satisfied. Figure 7 shows both arrangements of fibres: square and hexagonal, with a 30% SiC volume fraction. The stress level required to cause damage at the interface is 64.75 MPa and 62.97 MPa for a square and hexagonal arrangements, respectively, at room temperature. The composite material, with square arrangement, undergoes longer elongation than a composite with hexagonal arrangement, before damage appears at the interface between fibre and matrix.

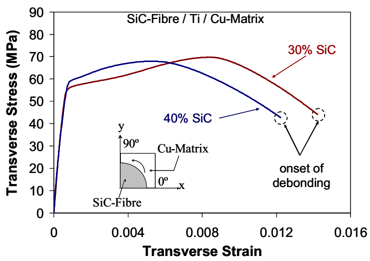

Figure 6. Transverse stress-transverse strain: 30 and 40% of SiC_f at 20 ºC

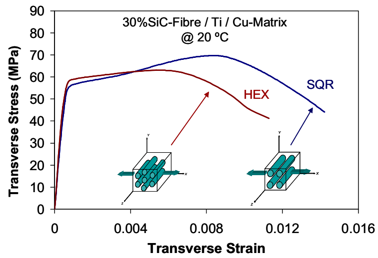

Figure 7. Effect of fibre arrangement in composite at room temperature (30% SiC_f)

Effect of temperature on transverse traction response. The onset of damage (when failure criterion is satisfied) appears when stresses reach 64.75 MPa and 52.32 MPa at 20 ºC and 550 ºC respectively (30% of SiC_f). After that, the stress decreases sharply. Additionally, the transverse strain (fracture elongation) of the composite is longer at 550ºC. Fig. 8 shows the stress-strain curve at 20 and 550 ºC for square fibre arrangement. On the other hand, fig. 9 shows the behaviour of the composite at 550ºC with 30 and 40% of volume fractions of SiC (square arrangement). The composite, reinforced with 30% of SiC fibre, presents a longer fracture elongation. The separation between the fibre and the matrix starts at 18 and 9 degrees for a volume fraction of 30 and 40% of SiC fibre, respectively. As shown in fig. 10, the composite, with hexagonal arrangement of fibres, undergoes more plasticity before the interface starts to debond. On another hand, the zone of interface debonding ranges from 0º to 16º for copper matrix composite (with hexagonal arrangement) when subjected to 550 ºC, as shown in figure 10.

Summary The initial damage can be located through radial tensions. The separation of the interface starts at 0 degrees and from 0º to 27º for a composite with square and hexagonal arrangement, respectively, both with a 30% volume fraction of fibres. Debonding zone decreases from 0 to 16 degrees when the temperature increases from room temperature to 550 ºC. But, the tensile radial stresses generated, during the heating, are not enough to induce separation in the interface. Afterwards, transverse loading is applied, thus the debonding interface starts at 9 and 18 degrees for a composite with 40 and 30% volume fractions, respectively (for a square arrangement). Similar interface behaviour can be observed for a hexagonal arrangement of fibre, where interface debonding is located from 0 to 16 degrees at 550ºC.

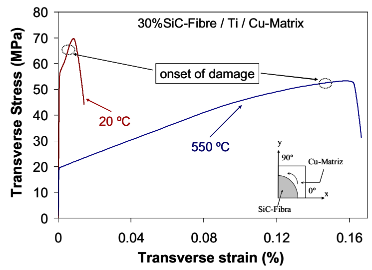

Figure 8. Stress-strain curve at 20 and 550 ºC

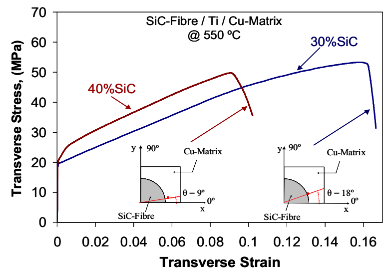

Figure 9. Transverse stress-strain curve of composite at 550ºC, with 30 and 40% of volume fraction of SiC (square array)

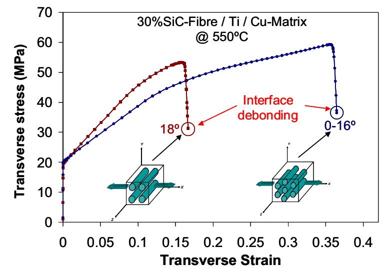

Figure 10. Transverse stress-strain curve of composite at 550 ºC, with 30% of volume fraction (sqr. and hex. arrays)

Acknowledgements The authors wish to acknowledge the founds to EXTREMAT project (contract no. NMP3-CT-2004-500253) and from the Spanish Ministry of Education and Science, for their financial support (project MAT2004-01227). Alfredo Ríos' contract is funded by the Spanish Ministry of Education within the framework of Torres Quevedo Programme, and co-funded by the European Social Fund.

References

[1] Fietziek, H., Specification of user requirements on Heat Sink Materials for Luncher Propulsion. Internal communication. EXTREMAT Project, 2005.

[2] McLean, M., Creep deformation of metal--matrix composites. Composites Science and Technology, 1985. 23(1): p. 37-52.

[3] Marshall, D.B., W.L. Morris, B.N. Cox, J. Graves, J.R. Porter, D. Kouris, and R.K. Everett, Transverse strengths and failure mechanisms in Ti3Al matrix composites. Acta Metallurgica et Materialia, 1994. 42(8): p. 2657-2673.

[4] Akser, E.O. and K.-L. Choy, Finite element analysis of the stress distribution in a thermally and transversely loaded Ti-6Al-4V/SiC fibre composite. Composites Part A: Applied Science and Manufacturing, 2001. 32(2): p. 243-251.

[5] Chawla, K.K., Thermal fatigue damage in Borsic Al(6061) composites. Journal of Materials Science Letter, 1976. 11: p. 1567-1569.

[6] Yoda, S., N. Kurihara, K. Wakashima, and S. Umekawa, Thermal cycling-induced deformation of fibrous composites with particular reference to the tungsten-copper system. Metallurgical Transactions A (Physical Metallurgy and Materials Science), 1978. 9A(9): p. 1229-1236.

[7] Zywicz, E. and D.M. Parks, Thermo-viscoplastic residual stresses in metal matrix composites. Composites Science and Technology, 1988. 33(4): p. 295-315.

[8] Wilkinson, A.J., Interfacial stresses in a continuous fibre metal matrix composite. Scripta Metallurgica et Materialia, 1992. 26(3): p. 387-392.

[9] Shaw, L.L. and D.B. Miracle, Effects of an interfacial region on the transverse behavior of metal-matrix composites--A finite element analysis. Acta Materialia, 1996. 44(5): p. 2043-2055.

[10] Nimmer, R.P., Fiber-matrix interface effects in the presence of thermally induced residual stresses. Journal of Composites Technology & Research, 1990. 12(2): p. 65-75.

[11] Nimmer, R.P., R.J. Bankert, E.S. Russell, G.A. Smith, and P.K. Wright, Micromechanical modeling of fiber/matrix interface effects in transversely loaded SiC/Ti-6-4 metal matrix composites. Journal of Composites Technology & Research, 1991. 13(1): p. 3-13.

[12] Li, D.S. and M.R. Wisnom, Factors controlling the transverse tensile properties of unidirectional SiC/Ti-6Al-4V. Composites Engineering, 1995. 5(3): p. 235-255.

[13] Wisnom, M.R., Factors affecting the transverse tensile strength of unidirectional continuous silicon carbide fibre reinforced 6061 aluminium. Journal of Composite Materials, 1990. 24(7): p. 707-726.

[14] Li, D.S. and M.R. Wisnom, Micromechanical modelling of SCS-6 fibre-reinforced Ti-6Al-4V under transverse tension-effect of fibre coating. Journal of Composite Materials, 1996. 30(5): p. 561-588.

[15] Ding, W. and P. Bowen, Micromechanical modeling of unidirectional continuous sigma fiber-reinforced Ti-6Al-4V subjected to transverse tensile loading. Metallurgical and Materials Transactions A: Physical Metallurgy and Materials Science, 2002. 33(9): p. 3045-3054.

[16] Zhang, H., K.T. Ramesh, and E.S.C. Chin, Effects of interfacial debonding on the rate-dependent response of metal matrix composites. Acta Materialia, 2005. 53(17): p. 4687-4700.

[17] Aghdam, M.M. and S.R. Falahatgar, Micromechanical modeling of interface damage of metal matrix composites subjected to transverse loading. Composite Structures. Twelfth International Conference on Composite Structures, 2004. 66(1-4): p. 415-420.

[18] Balasivanandha Prabu, S., L. Karunamoorthy, and G.S. Kandasami, A finite element analysis study of micromechanical interfacial characteristics of metal matrix composites. Journal of Materials Processing Technology. Proceedings of the International Conference in Advances in Materials and Processing Technologies, 2004. 153-154: p. 992-997.

[19] Chandra, N. and C.R. Ananth, Analysis of interfacial behavior in MMCs and IMCs by the use of thin-slice push-out tests. Composites Science and Technology, 1995. 54(1): p. 87-100.

[20] ABAQUS, Versión 6.5-1. Hibbitt, Karlsson and Sorensen Inc. 2004.

[21] Turon, A., P.P. Camanho, J. Costa, and C.G. Davila, A damage model for the simulation of delamination in advanced composites under variable-mode loading. Mechanics of Materials, 2006. 38(11): p. 1072-1089.

[22] Brendel, A., J. Woltersdorf, E. Pippel, and H. Bolt, Titanium as coupling agent in SiC fibre reinforced copper matrix composites. Materials Chemistry and Physics, 2005. 91(1): p. 116-123.

[23] Alfano, G. and M.A. Crisfield, Finite element interface models for the delamination analysis of laminated composites: Mechanical and computational issues. International Journal for Numerical Methods in Engineering, 2001. 50(7): p. 1701-1736.

[24] Camanho, P.P., C.G. Davila, and M.F. de Moura, Numerical Simulation of Mixed-Mode Progressive Delamination in Composite Materials. 10.1177/0021998303034505. Journal of Composite Materials, 2003. 37(16): p. 1415-1438.

[25] Osborne, D., N. Chandra, and H. Ghonem, Interphase behavior of titanium matrix composites at elevated temperature. Composites Part A: Applied Science and Manufacturing, 2001. 32(3-4): p. 545-553.